Electronic Supplementary Material (ESI) for Physical Chemistry Chemical Physics.

ELECTRONIC SUPPLEMENTARY INFORMATION

Weak nuclear spin singlet relaxation mechanisms revealed by experiment and computation

Boris Kharkov,[1] Xueyou Duan,[2] Jyrki Rantaharju,[3] Mohamed Sabba,[3]
Malcolm H. Levitt,[3] James W. Canary,[2] and Alexej Jerschow*[2]

[1] *Laboratory of Biomolecular NMR, St. Petersburg State University, St. Petersburg 199034, Russia*

[2] *Department of Chemistry, New York University, New York, NY 10003*

[3] *School of Chemistry, University of Southampton, Southampton, UK*

(Dated: March 6, 2022)

NMR DETERMINATION OF CHEMICAL SHIFT DIFFERENCE

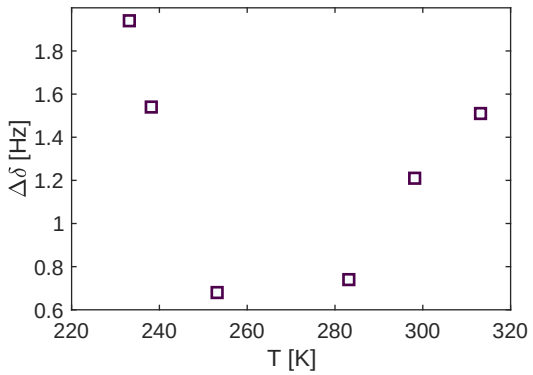

FIG. S1. Chemical shift difference between the vinylene protons, as inferred from the M2S seqeunce parameter optimization.

EVALUATION OF THE FAST MOTION REGIME ASSUMPTION

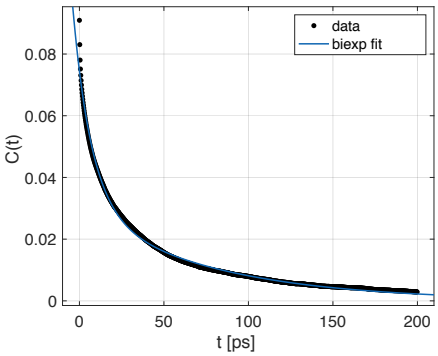

FIG. S2. Correlation function for the intermolecular ^{1}H-^{35,37}Cl dipolar coupling contribution to R_1 of the vinylene ^{1}H of the EPM molecule, along with a biexponential fit.

CONVERGENCE OF RELAXATION CALCULATIONS

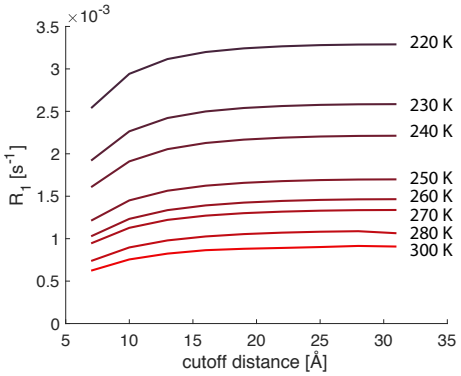

FIG. S3. R_1 relaxation rate constants for the intermolecular ^{1}H-^{35,37}Cl contribution as a function of cutoff distance.

DERIVATION OF THE SPIN-ROTATION RELAXATION EXPRESSION

The Hubbard model spin-rotation contribution to the R_1 relaxation rate constant for non-spherical molecules is given in Eq. (22) of Ref. [1]. For the axially symmetric case, expressed with the parallel and perpendicular friction constants $\epsilon_\parallel$ and $\epsilon_\perp$, respectively, the equation takes the form (see Eq. (18) of Ref. [1])

$$R_1^{sr} = \frac{2k_BT}{3\hbar^2}\left(I_\parallel^2 C_\parallel^2/\epsilon_\parallel + 2I_\perp^2 C_\perp^2/\epsilon_\perp\right), \tag{1}$$

where $I_\parallel$ and $I_\perp$ are the moments of inertia for rotation around the C-H bond, and perpendicular to it, respectively. The friction constants and diffusion constants $D_{\parallel,\perp}$ have the relationship (see Eq. (6.39) in Kowalewski and Mäler [2])

$$\epsilon_{\parallel,\perp} = \frac{k_BT}{D_{\parallel,\perp}}. \tag{2}$$

With these relationships, one obtains for the spin-rotation contribution

$$R_1^{sr} = \frac{2}{3\hbar^2}\left(I_\parallel^2 C_\parallel^2 D_\parallel + 2I_\perp^2 C_\perp^2 D_\perp\right). \tag{3}$$

CALCULATION OF CSA CONTRIBUTIONS TO R_1 AND R_S

The expressions for the R_1 component calculations are

$$R_1^{sym} = \frac{2}{15}(\omega_0\sqrt{3/2}||\sigma_{sym}||_F)^2\frac{\tau_2}{1+(\omega_0\tau_2)^2} \tag{4}$$

$$R_1^{anti} = \frac{1}{6}(\omega_0||\sigma_{anti}||_F)^2 \frac{\tau_1}{1+(\omega_0\tau_1)^2}. \quad (5)$$

Here, σ_{sym} and σ_{anti} designate the traceless symmetric and the antisymmetric tensor components, respectively, and $||\sigma||_F$ indicates the Frobenius norm of a tensor, i.e. the square root of the sum over the squares of all tensor elements. τ_2 is the second rank correlation time. For isotropic motion, one may assume that the first and second rank correlation times are related by $\tau_1 = 3\tau_2$. In the context of singlet-state relaxation, it was shown specifically that the antisymmetric component could become a major relaxation contribution [3]. In that work, the expressions for the R_S components were provided in the fast motion regime. Outside of that regime, the expressions become

$$R_S^{sym} = \frac{2}{9}(\omega_0||\Delta\sigma_{sym}||_F)^2 \frac{1}{5}(2\tau_2 + \frac{3\tau_2}{1+(\omega_0\tau_2)^2}) \quad (6)$$

$$R_S^{anti} = \frac{2}{9}(\omega_0||\Delta\sigma_{anti}||_F)^2 \frac{\tau_1}{1+(\omega_0\tau_1)^2}, \quad (7)$$

where $\Delta\sigma_{sym}$ and $\Delta\sigma_{anti}$ represent the symmetric and the antisymmetric components of the difference between the tensors at the two proton sites. For the R_1 calculations, the correlation time of the C-H bond vector reorientation was extracted from the MD trajectories. For the R_S calculations, the correlation time of the ^{1}H-^{1}H vinylene internuclear vector reorientation was used. These correlation times were obtained by calculating

$$a_1(t) = \cos(\theta(t)) \quad (8)$$

with the subscript 1 indicating the rank, and θ being the angle of the vector with respect to the z-axis. The k-th rank correlation function was calculated by

$$C_k(t) = \overline{a_k(t')^* a_k(t+t')}, \quad (9)$$

where the average was performed over t', and the correlation time was calculated by

$$\tau_k = \int_0^{t_{max}} C_k(t)/C_k(0). \quad (10)$$

The sum was performed over $t_{max} = 800$ ps.

From this result, the second-rank correlation time was calculated using $\tau_2 = \tau_1/3$ and used for the symmetric CSA interaction.

Fig. S4 shows the tensor norms for the conformations extracted from the MD trajectory. The CSA difference tensor norms were found to be $||\Delta\sigma_{sym}||_F = 4.35$ ppm and $||\Delta\sigma_{anti}||_F = 0.94$ ppm. The standard deviations were 0.13 and 0.18 ppm, respectively.

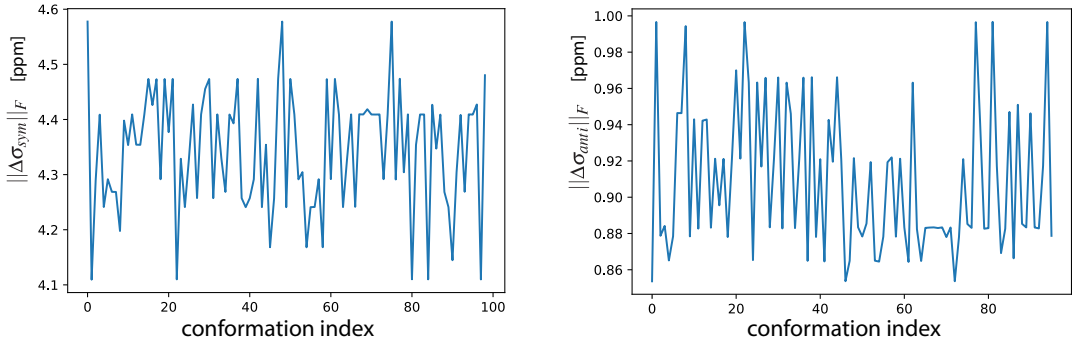

FIG. S4. Frobenius norms of the symmetric and antisymmetric components of the CSA difference tensors for the conformations extracted from the MD trajectory.

PARAMAGNETIC RELAXATION

A distance cutoff of 20 Å was used. The effective oxygen concentration needed to be evaluated over the volume ($\frac{4}{3}\pi r^3$), with r being the cutoff distance. When evaluated over the simulation box, the effective oxygen concentration was approximately 12 mM.

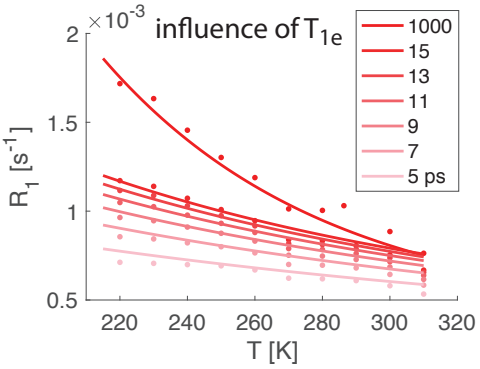

FIG. S5. The influence of T_{1e} on the contribution of oxygen to chloroform R_1.

VALIDATION OF COMPUTED R_1 RATES FOR EPM MOLECULE

Fig. S6 shows the experimental values for the R_1 rate constants determined for the vinylene protons of the EPM compound, along with the values obtained from MD simulations. No distinction between the rate constants for the two spins could be observed. The dominating mechanism for vinylene T_1 is the intra-pair dipolar coupling. Other mechanisms such as intra-molecular and intermolecular dipolar couplings, CSA relaxation, and the contribution of oxygen, can be shown to range from 1×10^{-3} s^{-1} to 5×10^{-3} s^{-1}, and are therefore approximately two orders of magnitude lower, and can hence be ignored in this calculation. As is seen in Fig. S6, the agreement between experiment and calculation is very good, providing confidence in the procedure. Furthermore, because the dominating mechanism has very few parameters (e.g. the distance between the protons is largely fixed), the observed correspondence between calculation and experiment also indicates that the reorientation correlation times calculated from MD trajectories must be fairly accurate over the observed temperature range.

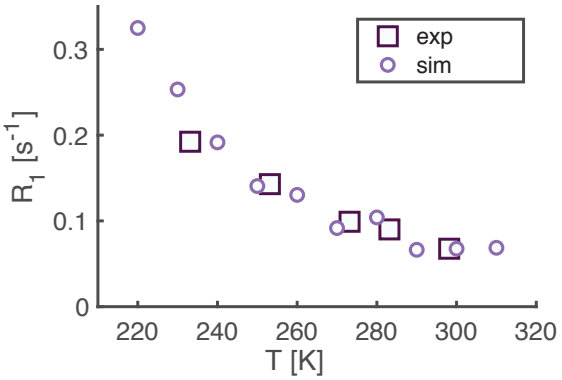

FIG. S6. Experimental (exp) and calculated (sim) R_1 rate constants for the vinylene protons in EPM.

[1] R. E. D. McClung, *Spin–Rotation Relaxation Theory*, Vol. 91 (John Wiley & Sons, Ltd, Chichester, UK, 2007).

[2] J. Kowalewski and L. Mäler, *Nuclear spin relaxation in liquids: theory, experiments, and applications*, 2nd ed. (CRC press, 2017).

[3] G. Pileio, J. T. Hill-Cousins, S. Mitchell, I. Kuprov, L. J. Brown, R. C. Brown, and M. H. Levitt, Long-lived nuclear singlet order in near-equivalent 13c spin pairs, J Am Chem Soc **134**, 17494 (2012).